Device Optimization and Application Study of low cost Printed Temperature Sensor for mobile and stationary battery based Energy Storage Systems

Joshua Grosch, Erik Teuber, Michael Jank, Vincent Lorentz, Martin März, Lothar Frey
Fraunhofer IISB, Erlangen, Germany
Joshua.Grosch@iisb.fraunhofer.de

***Abstract*— One of the most important physical parameters for state estimation in battery based Energy Storage Systems (ESS) is the temperature. This physical quantity does not only strongly influence state estimation for battery management systems, but also significantly affects lifetime and return on investment finally. Thus, monitoring the cell temperature is essential when high performance and efficiency is demanded. Contrary to this fact, less temperature sensors than battery cells are implemented in state of the art battery systems, to limit system costs. In this paper a low cost temperature sensor is presented. Based on printed electronics technology, a broad spectrum of designs and substrates is processable which leads to a variety of possible applications. After the selection of design and concept for battery applications, the processing of the sensor device is described. The main part of the paper is about the experimental validation of the printed temperature sensor performance. In a high power charge and discharge cycle of a single battery cell, the printed sensor is directly compared to state of the art temperature sensors implemented in mobile or stationary battery systems. Finally, the results are discussed and future perspectives are given. Both, the advantages and disadvantages of the printed temperature sensor are shown, whereas for the latter possible solutions are pointed out with respect to further developments.**

Keywords — temperature sensor; printed electronics; battery monitoring; state estimation; SOH; PTC; temperature gradient;

I. INTRODUCTION AND MOTIVATION

Nowadays, the big breakthrough of e-mobility has still not taken place. High costs and low range affect the competitiveness of EVs in a negative way. One of the most challenging tasks, to raise the EVs' attractiveness, is formed by the energy storage. By means of consistent research and development, ESS based on lithium ion battery cells have to become more lightweight, cheaper and, above all, more performant for the future. One possibility to enhance the performance of battery packs is a smart Battery-Management-System (BMS). Due to the combination of optimal battery load, temperature conditioning adjusted separately for every single battery cell and intelligent control algorithms, a maximum of efficiency can be achieved. Therefore the BMS needs precise information of every battery cell which is provided by special sensors. Amongst others, temperature sensors provide one of the most important information for estimating any battery state [7], e.g. State of Charge (SOC), State of Health (SOH) and State of Function (SOF), but also regarding safety and load de-rating features [6]. Thus, for an optimal state estimation of the ESS, the voltage and temperature of every single battery cell should be monitored. But high costs for the temperature sensor device itself and the wiring, connection and whole installation effort prevent this fact. The amount of installed temperature sensors in an ESS is far below the number of serial battery cells [8]. Another approach to determine the temperature of battery cells without any physical temperature sensor device is the sensor-less temperature measurement by using online impedance spectroscopy [1]. Using this method, the internal temperature of a battery cell is detected indirectly, while other techniques use special algorithms to estimate the internal temperature by attached temperature sensors on the surface of the battery cell [10]. The sensor-less procedure is a very interesting step towards future battery monitoring but still needs massive R&D until final realization. By reducing costs and implementation effort of temperature sensors the number of temperature monitoring devices could be increased. This directly enhances state estimation and finally the attractiveness of ESS. Within this paper, a low cost printed temperature sensor is presented. Because of its flat and compact design realized by special printing methods, it is possible to reduce both, implementation effort as well as overall costs.

II. MANUFACTURING OF THE SENSOR DEVICE

A. Selection of Sensor Concept and Type

The initial question when determining the concept of the temperature sensor for battery cells is about the attachment of the sensor to the battery cell in the most appropriate way. On the one hand, the sensor device can be directly printed on the battery cell housing and on the other each sensor is printed on its own, separate substrate. As low manufacturing costs are linked to high volume productions, the sensor and its manufacturing process should be suitable for every type of battery cell (pouch, cylindrical, prismatic etc.). Thus, every temperature sensor device will be printed on a separate substrate as a cross linked manufacturing process between battery cell and temperature sensor means both, an increasing complexity of the manufacturing and a lower level of freedom regarding sensor placement and connection. Thereby different arrangements of the sensor device are thinkable. They can be

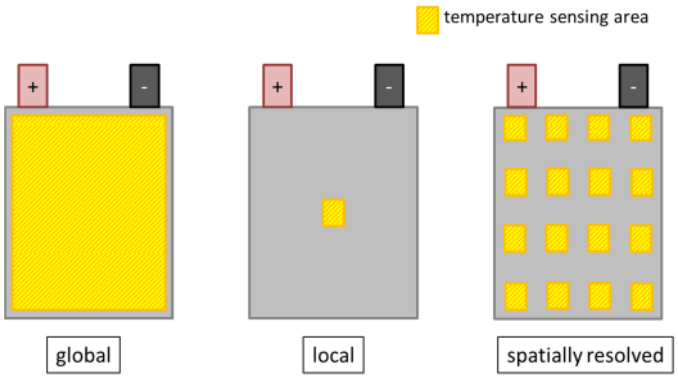


Fig.1: Schematic representation of different concepts for the temperature detection on the surface of a pouch-type battery cell. There is a differentiation between global, local and spatially resolved temperature sensing.

differentiated according to the type of detecting the cell temperature into global, local and spatially resolved temperature sensing, as shown in Fig.1. Global temperature detection of the battery cell means that the complete surface of one side of the cell is covered with the temperature sensor. That method gives an averaged value of the cells temperature as the temperature is measured across the entire area. Assuming that the battery cell shows inhomogeneous temperature distribution across the surface, there are one or more temperature gradients across the surface. The concept of global temperature sensing would detect the mean value of the cell temperature as all temperature gradients are averaged over the surface. Finally, no precise temperature measurement of the battery cell is possible. The bigger the sensor dimensions, the more inaccurate is the temperature detection. Moreover battery defects (e.g. dendrites), which result in local "hot spots" on the cell surface, are unlikely to be detected. Besides that aspect, the material costs of the temperature sensor are directly connected to the sensing area. Thus for large (global) area temperature detection, the material costs are high. Spatially resolved temperature detection of the battery cell means that an array of small sensor devices is arranged on the cell surface. Each device is a sensor detecting the temperature over just a small area. The surface of the battery cell is thereby divided into a grid. Each sensor detects the temperature of a single grid field. The grid is determined by the number of sensor elements which defines the resolution of the temperature detection. The spatially resolved method enables a very precise temperature measurement. Furthermore, every single temperature sensor device has to be addressable which results in high complexity as well as increased costs for the wiring and data interpretation of the sensor's resistance (e.g. by multiplexers). Another possible method for the detection of the temperature is local temperature sensing. This method requires knowledge about the temperature distribution of the stressed battery cell, as the temperature can only be measured at one spot of the battery cell. Local temperature detection makes sense, if information of the thermal behavior of the battery cell has already been gathered. If there is a known hot spot on the surface, the sensor device is just placed on that area fitting its dimensions. Besides the "single-point" temperature measurement and the required knowledge of the thermal behavior, the limitation of this method is that additionally evolving hot spots are not detectable. Abnormal behavior of the battery cell (e.g. due to operation beyond its limitations or inner defects) can result in the generation of new hot spots which are not detectable by local temperature sensing. A possible solution for this limitation may be the additional monitoring of the battery cell voltage combined with smart monitoring software. Additionally it is also thinkable to insert the sensor inside the cell housing. Therefore a special treatment for shielding the sensor device from the electrolyte needs to be developed which is not further discussed within the scope of this paper. As cost efficiency is a key aspect of the printed temperature sensor, the concept of local temperature detection is selected. Besides the concept of the temperature detection itself, the type of temperature sensor needs to be determined. State-of-the-Art temperature sensors applied for monitoring ESS are thermistors with positive (PTC) or negative (NTC) temperature coefficient of resistance (TCR), or thermocouples (TC). The main reasons for using thermistors in such applications are robust design and high durability amongst others. Due to the high thermal sensitivity of thermistors, the evaluation of the sensors regarding the electrical circuit is very simple. Therefore, this sensor type is mainly used in the end product (e.g. vehicles or stationary battery systems). The requirements for evaluating TCs are quite high but these sensors provide a more compact design, when compared to thermistors. Thus, TCs are mainly applied for prototype testing and laboratory examinations [2-3]. The aim of the printed temperature sensor, presented in this paper, is the combination of both, namely high TCR for easy evaluation and a flexible, compact design for easy implementation. Due to the low complexity, the available materials base, and the simple integration (printable, single device, no reference temperature needed, easily evaluable), the thermistor concept offers clear advantages over the thermocouple approach and is therefore chosen for implementation. However, the conventional PTC metal oxide sensors are either based on pearl-type packages or on high temperature rigid and rather thick ceramic substrates. Up to date, the commercial availability of temperature sensing materials for the development of customized layout and integration solutions is restricted to high temperature ceramic thick-film pastes and a few metallic materials offering only low TCR or low signal levels. By using printing electronics technology the aforementioned points can be realized by simple, cost-effective manufacturing (roll-to-roll printing) and the possibility to use flexible foils as substrate.

B. Placement of the temperature sensor

The placement of the temperature sensor(s) can be adapted to the system which has to be thermally observed and can comprise a single sensor placed at a known hot spot or of multiple sensors distributed over the battery cell surface (e.g. a sensor array). Knowing the maximum temperature of a battery cell has an essential importance for state estimation (SOC, SOH and SOF) and safety aspects (thermal runaway). The strategy for the optimum sensor placement is based on an IR temperature characterization of the pouch type battery cell while continuously discharging according to maximum operating conditions (Fig.3). The measurements show that the main temperature increase can be found below the cathode (positive electrode) of the battery. Thus, the most logical approach is to place a single temperature sensor device directly at the hot spot near the cathode contact.

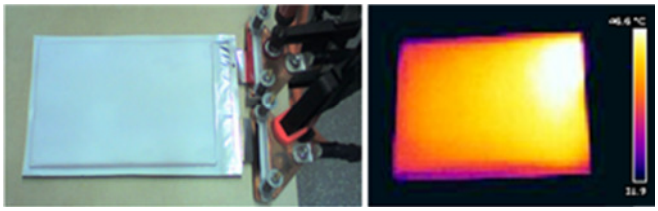


Fig.3**:** The battery cell was stressed under maximum load and the hot spot on the cell's surface was identified using an infrared camera**.**

C. Sensor Design

A planar design on flexible plastic foil consisting of three functional layers has been chosen which is fully realizable within inexpensive printed electronics technologies and materials for high volume production. The design of the demonstration sensor which is shown in Fig.2, is determined by the hot spot dimensions of the battery cell on the one hand and by the feasibility of the temperature sensor manufacturing on the other. The layers are each deposited in a separate printing process and stacked onto each other. The sensor is realized on a 150µm thick PET plastic substrate. A first screen printed layer from silver paste yields the wiring and contact metallization. On top of the electrodes, the temperature sensitive layer with a thickness of approximately 50µm is deposited, again by screen printing. The sensor fabrication is finalized by the application of an encapsulating layer that is intended to shield the sensor from moisture, contaminations and insulating it electrically. The thickness of the encapsulation is typically around 100µm. The chosen sensor architecture provides low complexity, high robustness and can be integrated with complementary devices on the same substrate for the realization of more complex sensor and control solutions. The overall thickness of the device is below 300µm. Regarding the substrate, the sensor is printed onto commercially available polyethylene terephthalate (PET) foils (HP 92296U) as initial experiments show that adhesion, film formation, and experimental parameters are suitable for the printing process. The sensitive material in our case is a polymer matrix filled with graphite particles. The principle of the temperature-induced change of resistance is the expansion and shrinking of the polymer with increasing/decreasing temperature. With expansion of the polymer, the graphite particles are separated from each other. This may lead to a reduction of interparticle contacts and result in an increasing resistance due to the loss of percolation paths along the current flow direction. For shrinking polymer with decreasing temperatures the principle applies vice versa. The wiring is used for contacting the sensitive element of the sensor. For the experiments a low-temperature curable screen printing paste by DuPont (DuPont 5064H) is used. This paste delivers a thicker silver layer and a considerably lower defect density than inkjet printed contacting lines. Silver inks are the current industry standard for printed conductor materials on low temperature substrates [9]. However, due to the expensive raw material, alternative materials like carbon, copper or aluminum are under investigation and are expected to enable a low-cost replacement of silver in the future. The encapsulation of the sensor was realized with a PET lamination foil (Ibico IB585036), due to very good cost-performance ratio and easy handling.

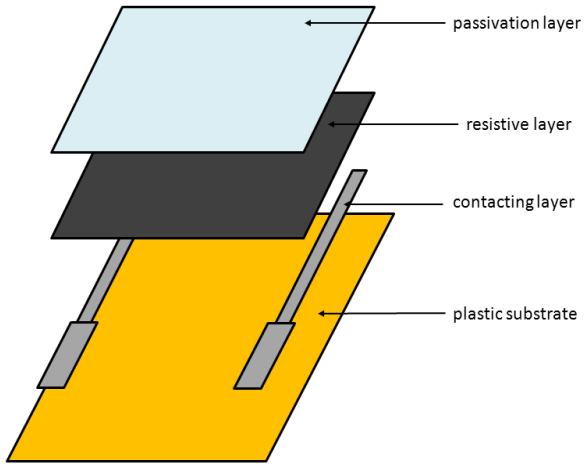


Fig.2: The figure shows the principal design of the printed temperature sensor which is adaptable to the thermal behavior of the battery cell.

D. Sensor Processing

The sensor is screen printed with a screen printing stencil that provides a polyester monofilament with a diameter of 48 µm and a 270 mesh. The squeegee is a diamond rubber type with 70 - 75 Shore A. The first layer to be printed on the PET foil is the silver (Ag) paste, which contacts the temperature sensitive material. The silver paste has a dynamic viscosity of 10 to 20 Pa·s and must be stirred for 2 minutes before printing directly onto the PET substrate material. The PTC paste (DuPont 7282) has a dynamic viscosity of 15 to 70 Pa·s at room temperature and can be printed without additional formulation. After each layer deposition, the substrate is cured on a hotplate at 140°C for 5 minutes to remove the organic solvents and the additives from the deposited material. For artificial aging, the samples are stored in the climate chamber for 110h at 65°C to drive solvent and water residues out of the layer. The aging cycle is interrupted after half of the processing time for the application of the passivation layer. Subsequently, the encapsulated sensor is aged for the remaining 55 h. The passivation is necessary to enhance the performance of the sensor, as will be shown later. Based on preliminary tests with several techniques for the sensor passivation by lamination or coating with polymers, the passivation with PET lamination foil is selected for the encapsulation of the temperature sensors. The lamination process with a foil leads to a thicker overall device but a good and tight passivation. Lamination is performed using an office-type lamination device, the lamination process itself is performed at ca. 100°C.

III. Experimental Description

A. Measurement Setup

The measurement setup consists of a climate chamber (type CTS T-70/50) which uses air circulation and a 16 channel USB data logger (type National Instruments NI USB-6210) connected to a PC for the measurement of the resistance of the sensors. The climate chamber and the 16 channel logger are controlled by a NI LabView program which is able to control and log the temperature of the climate chamber. Moreover, the sensor resistance is also logged at a high sampling rate. These values are displayed by the LabView program on a GUI. The achieved data is automatically stored in a log file for further

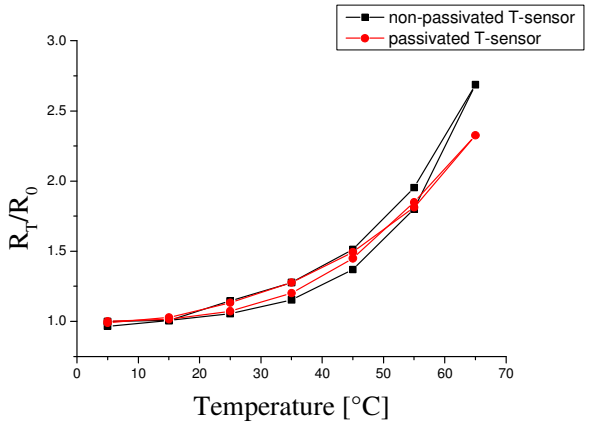


Fig.5: Characteristic (heating and cooling) curve of a non-passivated and passivated T-sensor. The encapsulation shows influence on both, hysteresis and TCR of the printed temperature sensor.

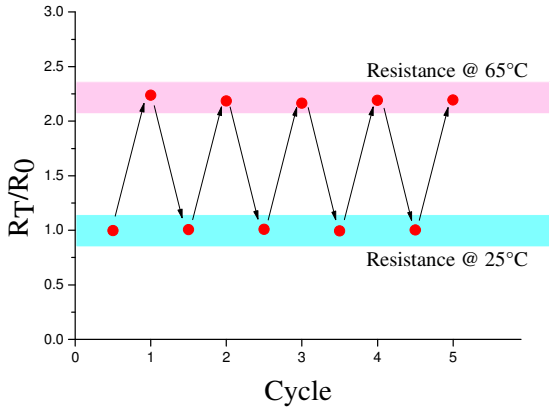


Fig.4: Cycling of the T-sensor from 25°C to 65°C to determine (short-term) ageing effects.

analysis. According to the main thermal operating area of battery cells, the temperature profile for the measurement starts at low temperatures (at 5°C) and sweep to 65°C (heating) and back (cooling). The used temperature profile corresponds to the thermal operation area of State-of-the-Art ESS [5].

B. TCR and Hysteresis

Thermistors change their resistance with temperature. This relation is linear approximated by the temperature coefficient of resistance (TCR).

$$TCR = \frac{R_{T1} - R_{T2}}{R_{max} \cdot (T_1 - T_2)} = \frac{\Delta R}{R_{max} \cdot \Delta T} \quad (1)$$

The values R_{T1}, R_{T2} are referred to the senor's resistance at a specific temperature T_1, T_2 (e.g. $T_1 = 25\ °C, T_2 = 30\ °C$). R_{max} is defined as the maximum value out of R_{T1}, R_{T2}. The information of the TCR is given in percent per Kelvin ($\%/K$) of temperature change. Another important quantity which is used to evaluate the performance of the temperature sensor is the hysteresis. This behavior is stated as the shift of the electrical resistance between heating and cooling phase of the characteristic curve.

$$Hysteresis = \frac{|R_{T_Heat} - R_{T_Cool}|}{R_{T_max}} = \frac{|\Delta R_T|}{R_{T_max}} \quad (2)$$

The values R_{T_Heat}, R_{T_Cool} are referred to the sensor's resistance at a specific temperature T for either heating (R_{T_Heat}) or cooling phase (R_{T_Cool}). R_{T_max} is defined as the maximum value out of R_{T_Heat}, R_{T_Cool}. The hysteresis is stated in %. The equations (1) and (2) will be used for the further characterization of the temperature sensor's performance regarding TCR and hysteresis.

IV. Measurement Results and Discussion

A. Effects of the Encapsulation

Basically, encapsulation means the generation of an inert surface on the material. That can be achieved by depositing an impermeable, protective layer (e.g. of liquid or solid polymer) on top of the temperature sensitive material. The protection layer is minimizing external impacts of potential reactants on internal material reactions. Encapsulating the T-sensor device shows a strong influence on its characteristics, namely hysteresis and TCR, as can be seen in Fig.5. Two different versions of the printed temperature sensor, namely a passivated and a non-passivated version, are evaluated in the temperature range from 5°C to 65°C. The electrical resistance of the sensors is recorded over the temperature for both, heating from 5°C to 65°C and cooling from 65°C to 5°C, to identify hysteresis behavior. For comparison reasons, the absolute values of the measured T-sensor resistance are standardized to R_0 which is the T-sensor resistance at 5°C. R_T is the resistance at temperature T. Referred to Table 1, passivating the T-sensor according to the procedure mentioned before reduces hysteresis effects from 6.41% to 3.09% which is less than a half of the originally values. Regarding the TCR, the impact of the passivation also shows a slight reduction from 1.49%/K to 1.29%/K. For better comparison reasons, the values shown in Table 1 are averaged over the whole temperature range from 5°C to 65°C. The values of the TCR and hysteresis are calculated according to equation (1) and (2), which have been described before. Furthermore it can be seen, that the TCR of the sensor peaks between 50°C to 65°C, which means that the highest accuracy is provided in this temperature range. At temperatures below 20°C the accuracy is significantly lower. These temperature sensor characteristics correspond to the thermal operating area of most lithium ion battery cells, where the maximum temperature is between 50 to 60°C and the minimum temperature is between 0 to 20°C, which makes the chosen material even more suitable for this kind of applications.

Table 1: Evaluation of encapsulation impact regarding the performance of the T-sensor

T-sensor	**Performance**	
	Hysteresis	***TCR***
Non-passivated	6.41%[1]	1.49%/K[1]
Passivated	3.09%[1]	1.29%/K[1]

[1] averaged value

B. Ageing of the T-sensor

Another important property which has to be determined is the sensor stability. A reason for the instability of the temperature sensor device could be an insufficient encapsulation of the thermal sensitive layer which would lead to an ageing process of the used resistive material. This means there would be fluctuating values of the temperature sensor's electrical resistance at equal temperature levels. To examine this effect, the temperature sensor is cycled from 25°C to 65°C and the electrical resistance is measured. It can be seen in Fig.4 that the there is almost no fluctuation of the T-sensor's resistance values which means that the encapsulation of the resistive material is acceptable. For a full investigation of sensor ageing effects, one has to distinguish between short- and long-term effects which affect the sensor performance. The measurement shown in Fig.4 shows the short-term behavior of the sensor stabitility, which seems to be acceptable for the performed cycle number of 5. In order to determine long-term ageing effects, further investigations need to be done which means expansion of the collection of data and thus are planned for the future.

C. Evaluation against commercial T-sensors

In order to determine the performance of the printed temperature sensor, the device is directly compared to other commercial available temperature sensors. The printed T-sensor is attached on the one extensive side of a prismatic battery cell, a type K thermocouple and an EPCOS NTC (type B57861S0103F045) on the other. All sensors are mounted on the same location of the surface of the battery cell to ensure similar cell temperatures. A symmetrical temperature spread of the inner battery cell temperature is assumed. The battery cell is stressed with an H&H battery cycler at stated maximum ratings of 8C to ensure a strong increase of the cell temperature, which limits the charge and discharge current to 160A. The whole measurement setup is placed on a thermally insulating foil on a laboratory desk with an ambient room temperature of 23°C. Thus, it can be assumed that natural convection is the dominating heat transfer mechanism. For the duration of the battery cell cycling and relaxation, the temperature is logged by the different temperature sensor devices. The results can be seen in Fig.6. For the duration of T_1=230s the battery cell is charged at 160A, until the charge voltage limit of 2.6V is reached and the charging mode is switched from constant current to constant voltage. Thereby the charge current is slowly decreased which results in a descending rise of the cell temperature compared to the constant current charge. At T_2=413s, the cell is discharged completely at 160A while the temperature of the battery cell is continuously increasing until almost 60°C is reached in the end at T_3=795s. Afterwards, the battery cell is thermally and electrically relaxating until the end of measurement at ca. 5200s. The course of the measured temperature values of every sensor seems similar when compared to each other. However some deviations of the printed sensor can be seen. For a more precise determination of the temperature difference, both, NTC and the printed sensor, are referenced to the TC which is therefore stated as the reference sensor. It can be seen that the NTC shows a relatively equal deviation between 0 and 1 K over the whole measurement duration. Further it can be seen that the deviation of the printed sensor is between 2 and 3 K at the start and end of the measurement, which can be attributed to an offset error. The reason of this error can be derived from an improper calibration of the used temperature versus resistance table for the printed sensor or due to hysteresis effects. While charging the battery cell it can be seen that $\frac{\partial T_{cell}}{\partial t}$ of the cell temperature T_{cell} has its maximum. The thermal reaction time of the TC and NTC are very similar but the printed sensor provides a lower reaction time which can be explained by the higher reaction time of the printed sensor due to a higher thermal mass. The size of the sensing area of the printed sensor is 1cm², while the sensing area of both, the NTC and TC, is negligible small. When the cell temperature reaches 45°C, the reaction time of the printed sensor is much higher compared to the other sensors. Thus, the temperature dependent reaction times of the printed sensor are rather linked to the nonlinear properties of the sensor material. Finally, the measured temperatures of every sensor are similarly slowly descending until the battery cell temperature reaches room temperature. Furthermore it can be seen, that the printed sensor material seems to be far more susceptible to fluctuations than the NTC which results in noisy measurement values for the temperature deviation. The noise becomes stronger while the battery is cooling down which can be referred to the inhomogeneous shrinking of the temperature sensitive polymer matrix described before in chapter II.C.

D. Contacting the temperature sensor device

For the investigations performed in this paper, the printed temperature sensor has been contacted by standard 0.35mm² stranded wires with M4 ring cable lugs screwed to the sensor device. This type of contacting was chosen for its high reliability, easy realisability and low complexity as the focus of this work is not on innovative connection solutions for printed electronics. For further developments into this direction a whole variety of possibilities are thinkable. Several temperature sensors can be deposited on a shared flexible substrate which is installed meander shaped through the battery stack. Every sensor has a separate contacting layer which is joined at one end of the substrate. Both, a wired and wireless connection are possible. The wired connection from the substrate foil to the monitoring or evaluation electronics can be done by a suitable connector (e.g. foil connector or contact springs). The wireless connector could be realized by a separate evaluation circuit on the shared flexible substrate of the temperature sensors which communicates the data via radio transmission to the BMS.

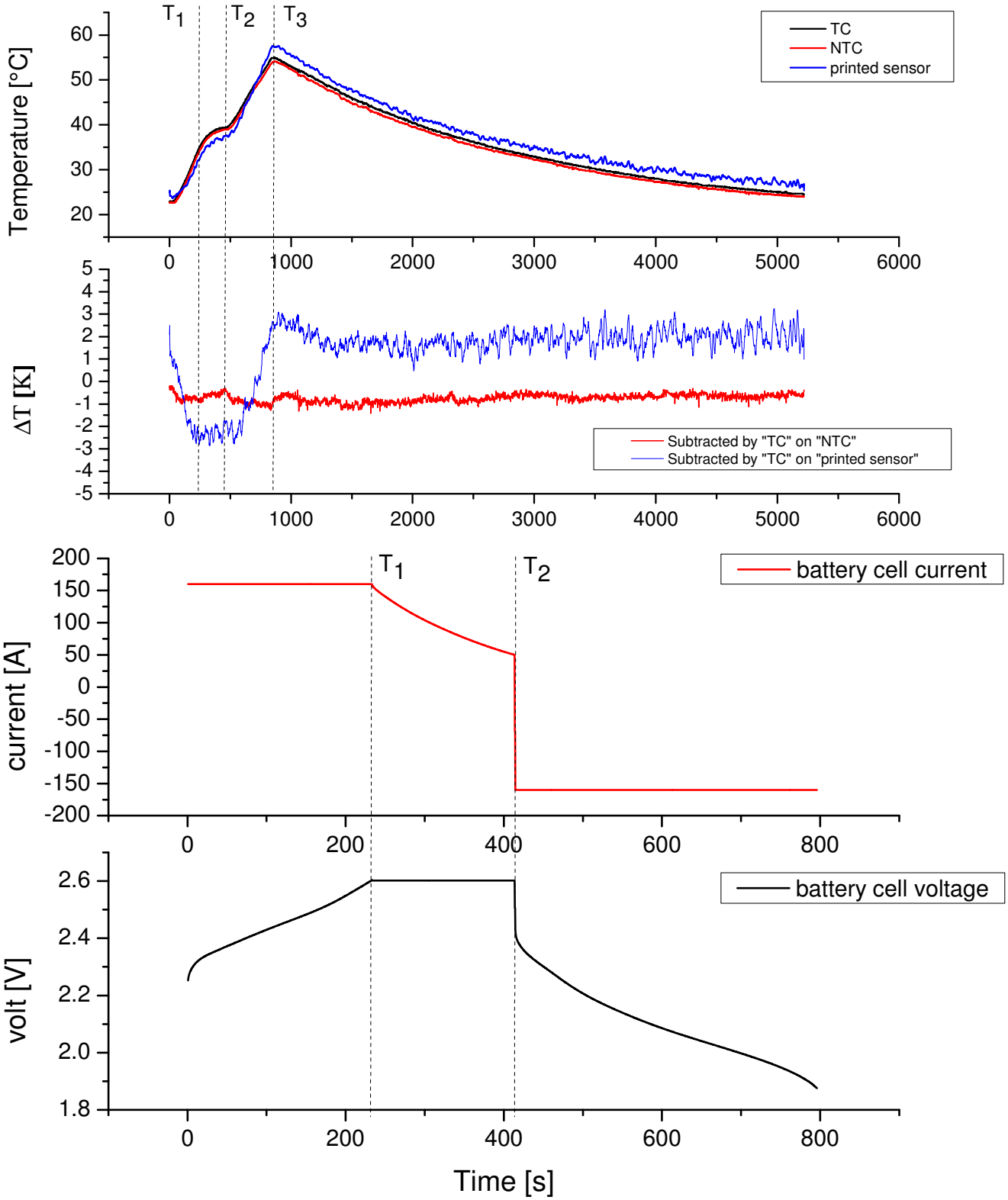


Fig.6: The printed temperature sensor is evaluated against SotA temperature sensors. The first graph shows the course of the absolute cell temperature measured by every sensor while the second graph shows the temperature deviation between the thermocouple and NTC respectively printed sensor. Third and fourth graph show battery cell voltage and charge/ discharge current. For better demonstration, the time scale of the last two graphs have been adapted.

V. Conclussion and Outlook

In this paper, a novel printed temperature sensor is presented which is a low cost alternative to existing NTC temperature sensor e.g. used for monitoring battery systems. The design of the printed sensor basically consists of the additive deposition of functional materials solely and is therefore predestinated for high volume roll-to-roll production. Furthermore, the low complexity of the sensor manufacturing provides a high grade of reproducibility, also the used materials are widely spread and commonly available. Regarding the performance, the temperature sensor provides a high TCR and an ultra-flat form factor below 300µm. Moreover it can be seen that encapsulating the device significantly reduces hysteresis effects but simultaneously show low impacts on the TCR. Thus, the encapsulation increases the sensor performance and also ensures a low ageing process as shown. Compared to State-of-the-Art temperature sensor, the printed sensor does not meet a similar accuracy in its current stadium. By means of consistent further development of the sensor design and calibration this point will be enhanced. Especially regarding contacting techniques there are a lot of possibilities which will be pursued in further publications. Using the presented temperature sensor device instead of standard commercial available NTC solutions for battery monitoring issues, the material and implementation costs can be significantly reduced. Thus, if there is a smaller amount of installed temperature sensors than battery cells in the ESS, the number of temperature sensors can be increased at the same level of costs. This will enable a higher accuracy of battery state estimation as a printed temperature sensor can be applied for every single battery cell. Due to the simple design and usage of low cost material of the printed sensor, it is imaginable to successively extent the amount of temperature sensing device per battery cell. The aim of ongoing research is to develop a temperature sensor array, consisting of an n x n matrix of printed sensor devices, at marginal rising costs. Using a sensor array, the temperature gradient of every single battery cell can be detected which will further increase the performance of the whole battery system as the accuracy of the state estimation is further increased. Another interesting approach for future investigations is the integration of the presented printed temperature sensor into battery cells. Measuring the inner temperature of a battery cell will further enhance battery diagnostics, as there is a difference when measuring the cell temperature inside or outside the encasement [4]. To place the printed sensor inside a battery cell, the encapsulation has to be resistant against the electrolyte, which will need further research activities. The general device layout of the printed temperature sensor can be utilized for a range of passive device concepts that may extend a modular BMS, e.g. for balancing resistors, heaters, or chemical sensors for humidity measurement. The base function of these additional devices can be realized by replacing the sensitive layer by an alternative functional material and adapting the layout.

Acknowledgment

The research leading to these results has received funding as part of the European Union Seventh Framework Program (FP7/2007-2013) under grant agreement n°285224 (“SuperLIB”).

References

[1] L.H.J. Raijmakers, D.L. Danilov, J.P.M. van Lammeren, M.J.G. Lammers, P.H.L. Notten, “Sensorless battery temperature measurements based on electrochemical impedance spectroscopy” in Journal of Power Sources 247 (2014), pp. 539-544.

[2] Madhu Santosh K. Mutyala, Jingzhou Zhao, Jianyang Li, Hongen Pan, Chris Yuan, Xiaochun Li, “In-situ temperature measurement in lithium ion battery by transferable flexible thin film thermocouples” in Journal of Power Sources 260 (2014), pp. 43-49.

[3] Zhe Li, Jianbo Zhang, Bin Wu, Jun Huang, Zhihua Nie, Ying Sun, Fuqiang An, Ningning Wu, “Examining temporal and spatial variations of internal temperature in large-format laminated battery with embedded thermocouples” in Journal of Power Sources 241 (2013), pp. 536-553

[4] Christophe Forgeza, Dinh Vinh Do, Guy Friedrich, Mathieu Morcrette, Charles Delacourt, “Thermal modeling of a cylindrical LiFePO4/graphite lithium-ion battery” in Journal of Power Sources 195 (2010), pp. 2961–2968.

[5] Gi-Heon Kim, Jeffrey Gonder, Jason Lustbader and Ahmad Pesaran, “Thermal Management of Batteries in Advanced Vehicles Using Phase-Change Materials” in The World Electric Vehicle Journal, Volume 2, Issue 2 (2008), pp. 0134-0147

[6] Siddique A. Khateeb, Shabab Amiruddin, Mohammed Farid, J. Robert Selman, Said Al-Hallaj, “Thermal management of Li-ion battery with phase change material for electric scooters: experimental validation” in Journal of Power Sources, Volume 142, Issues 1–2, 24 March 2005, pp. 345–353

[7] Brandl, M.; Gall, H.; Wenger, M.; Lorentz, V.; Giegerich, M.; Baronti, F.; Fantechi, G.; Fanucci, L.; Roncella, R.; Saletti, R.; Saponara, S.; Thaler, A.; Cifrain, M.; Prochazka, W., "Batteries and battery management systems for electric vehicles," *Design, Automation & Test in Europe Conference & Exhibition (DATE), 2012* , vol., no., pp.971,976, 12-16 March 2012, doi: 10.1109/DATE.2012.6176637

[8] M. Wenger, R. Waller, V.R.H. Lorentz, M. März, M. Herold, „Investigation of gas sensing in large lithium-ion battery systems for early fault detection and safety improvement” IECON 2014, 29 October-1 November 2014

[9] S. Merilampi, T. Laine-Ma, P. Ruuskanen, “The characterization of electrically conductive silver ink patterns on flexible substrates”, Microelectronics Reliability 49 (2009), pp. 782–790

[10] Ienkaran Arasaratnam, Jimi Tjong, Ryan Ahmed, Mohammed El-Sayed and Saeid Habib, “Adaptive Temperature Monitoring for Battery Thermal Management”, Transportation Electrification Conference and Expo (ITEC), 16-19 June 2013